Light-Harvesting Using High Density *p*-type Single Wall Carbon Nanotube/ *n*-type Silicon Heterojunctions

Zhongrui Li,[†,*] Vasyl P. Kunets,[‡] Viney Saini,[†] Yang Xu,[†] Enkeleda Dervishi,[†] Gregory J. Salamo,[‡] Alexandru R. Biris,[§] and Alexandru S. Biris[†,*]

[†]Nanotechnology Center, University of Arkansas at Little Rock, Arkansas, 72204, [‡]Physics Department, University of Arkansas, Fayetteville, Arkansas, 72701, and [§]National Institute for Research and Development of Isotopic and Molecular Technologies, P.O. Box 700, R-400293 Cluj-Napoca, Romania

ABSTRACT Photovoltaic conversion was achieved from high-density *p*—*n* heterojunctions between single-wall carbon nanotubes (SWNTs) and *n*-type crystalline silicon produced with a simple airbrushing technique. The semitransparent SWNT network coating on *n*-type silicon substrate forms *p*—*n* heterojunctions and exhibits rectifying behavior. Under illumination the numerous heterojunctions formed between substrate generate electron—hole pairs, which are then split and transported through SWNTs (holes) and *n*-Si (electrons), respectively. The nanotubes serve as both photogeneration sites and a charge carriers collecting and transport layer. Chemical modification by thionyl chloride of the SWNT coating films was found to significantly increase the conversion efficiency by more than 50% through adjusting the Fermi level and increasing the carrier concentration and mobility. Initial tests have shown a power conversion efficiency of above 4%, proving that $SOCl_2$ treated-SWNT/*n*-Si configuration is suitable for light-harvesting at relatively low cost.

KEYWORDS: *p*-type SWNT · *p*—*n* heterojunction · *n*-type Si · photovoltaic device · thionyl chloride

Carbon nanotubes (CNTs) possess unique electrical and optical properties that make them an ideal candidate for various components in modern electronics.[1,2] These superior properties of CNTs also allow them to be useful materials in highly active photovoltaic devices. Photovoltaic effect can be achieved in ideal carbon nanotube diodes.[3] Individual single-wall carbon nanotubes (SWNT) can form an ideal *p*—*n* junction diode. Under illumination, the SWNT diode demonstrates significant power conversion efficiencies owing to the enhanced properties of an ideal diode. In organic solar cell applications, the CNTs are mainly used as nanoscale fillers for polymer matrices or as transparent electrodes for collecting charge carriers.[4,5] The high aspect ratios and large surface area of nanotubes could be beneficial to exciton dissociation and charge carrier transport thus improving the power conversion efficiency for polymer-based photovoltaics. The conjugated polymers (*e.g.*, P3HT) produce excitons under illumination, while nanotubes embedded into the polymer matrix only provide more interfacial area for exciton dissociation and charge transport path.[6] However, donor—acceptor type structures consisting of conjugated polymers mixed with nanotubes still suffer low conversion efficiency.[7] Further, phase segregation between nanotubes and polymers, aggregation of nanotubes at higher concentration, and coexistence of metallic and semiconducting nanotubes are major limiting factors to the device fabrication and performance. Additionally, nanotube films used as transparent electrodes have shown negligible improvement in efficiency compared with ITO glass.[8]

In the solar cell industry, the semiconductor heterostructures are widely utilized to harvest light energy. In this work, we have designed and tested simple photovoltaic devices based on the heterojunctions between *n*-type semiconductor (*n*-Si) and carbon nanotubes (Figure 1a). SWNTs served as both photogeneration sites and a charge carriers collection/transport layer. SWNTs were utilized because of their many advantages over multiwall carbon nanotubes, such as a wide range of direct bandgaps matching the solar spectrum,[9,10] strong photoabsorption from infrared to ultraviolet,[11,12] high carrier mobility,[13] and reduced carrier transport scattering.[14] The solar cells consisted of a semitransparent thin film of nanotubes conformally deposited on an *n*-type crystalline silicon substrate to create high-density *p*—*n* heterojunctions between nanotubes and *n*-Si substrate which favor charge separation and extract electrons and holes. Here Si was selected because of its well-developed industrial applications and good electrical

*Address correspondence to zxli3@ualr.edu, asbiris@ualr.edu.

Received for review February 26, 2009 and accepted May 12, 2009.

Published online May 20, 2009.
10.1021/nn900197h CCC: $40.75

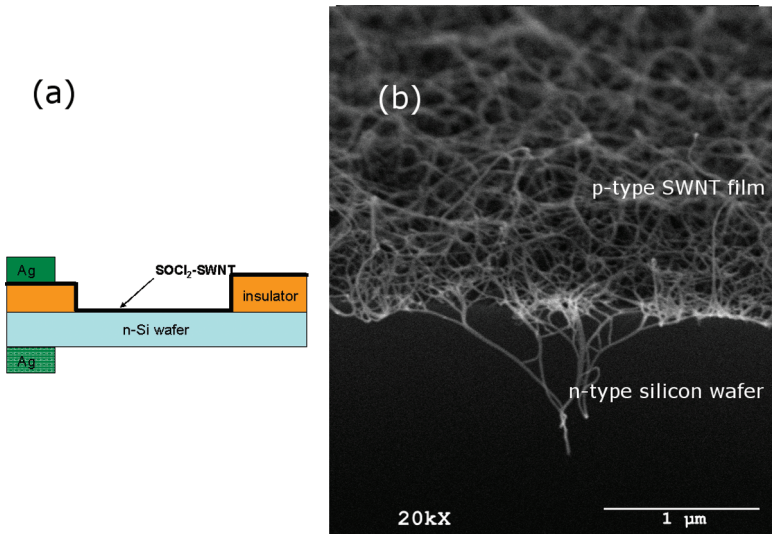

Figure 1. (a) Schematic diagram of a SWNT/n-Si solar cell. (b) SEM image of a SWNT film showing porous network structure, SWNT bundles in close contact to the *n*-Si surface.

performance in solar cells. Furthermore, the post-treatment of SWNT coating films with thionyl chloride ($SOCl_2$) can considerably improve the photovoltaic properties of the heterogeneous junctions.

RESULTS AND DISCUSSION

Effect of SWNT Coating Thickness on Photovoltaic Performance. The morphology of these coatings can be described as a randomly distributed network of SWNTs. SEM characterization revealed a porous network structure of the airbrushed SWNT film that is virtually free of catalyst residue or amorphous carbon particles (Figure 1b). The SWNTs lying on the substrate surface form numerous heterojunctions in contact with the underlying n-type Si substrate. The networks of SWNTs form agglomerates of nanotube bundles containing many well-aligned tubes alternating with empty regions. Therefore, it is difficult to define the thickness of these networks. Optical transmission was chosen as an appropriate method of averaging the structural irregularities and characterizing the thickness of various thin SWNT networks prepared on a glass substrate. As seen in Figure 2, two structures, (6,5) and (7,5) dominate the semiconducting nanotube distribution and comprise more than half of the population.[15] The transmittance values measured on our five transparent networks at wavelength of 550 nm are given in the inset of Figure 2. The film thickness can be controlled to reach hundreds of nanometers by using different numbers of airbrushing strokes. Such semitransparency ensures the absorption of the solar light by both the SWNT film and the underlying Si wafer. Our SWNT samples were complexes of conductive and semiconductive type of SWNTs. Four-probe measurements for the SWNT films showed that the sheet resistance for our SWNT films varied from 250 to 3900 Ω/sq for SWNT films with a transmittance of 51−86% at wavelength of 550 nm. Thus, our SWNT films can be directly used as a transparent conductive layer for solar cells, and this can help simplify the fabrication of the CNT solar cells.

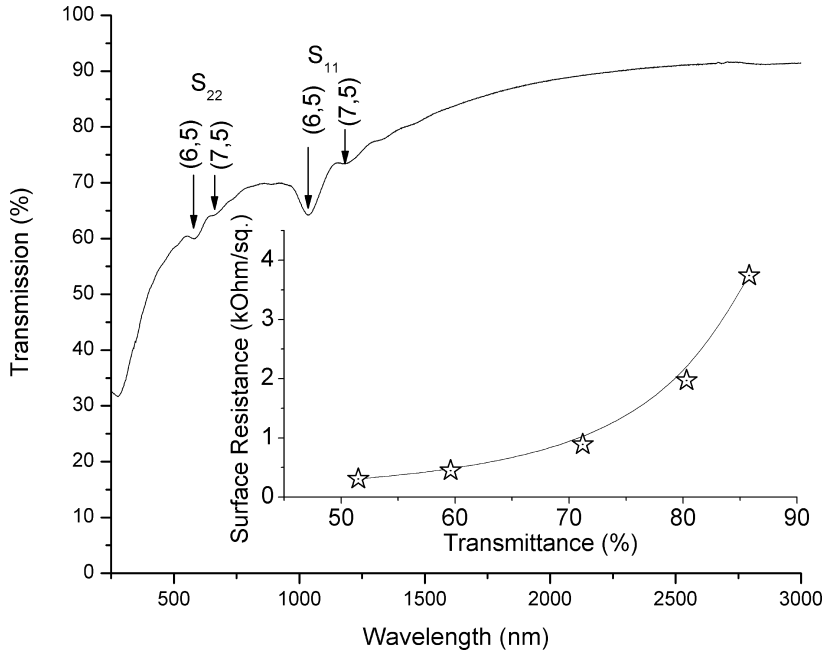

Figure 2. Optical transmission property of a SWNT reference film. The arrows S_{11} and S_{22} mark the absorptions related to the electronic transitions between pairs of van Hove singularities in the semiconducting tubes (6,5) and (7,5). Two structures, (6,5) and (7,5) together dominate the semiconducting nanotube distribution and comprise more than half of the population. Inset: Optoelectronic performance of SWNT films with different thickness at wavelength of 550 nm.

Figure 3a shows the current−voltage characteristics of a typical SWNT/*n*-Si solar cell, in which the SWNT film has about 57% transmittance (at 550 nm) under dark and white light illumination (AM1.5, ~100 mW/cm^2). The device revealed evident *p*−*n* junction behavior under dark light. The reversed current density was very low (~30 μA/cm^2) when the bias voltage was ramped from −1.0 to 0 V. This value is almost 400 times smaller than the forward current density (~13 mA/cm^2 at 1.0 V). Under illumination, the *I*−*V* curve shifts downward, with an open-circuit voltage V_{oc} and short-circuit current density J_{sc} of about 0.5 V and 21.8 mA/cm^2, respectively. While the value of V_{oc} is comparable to previous reports based on P3HT-SWNT composite structures, the J_{sc} of this SWNT/*n*-Si solar cell without polymer (P3HT) addition has been enhanced over 60 times more than that of the composite cells (0.34 mA/cm^2).[16]

The dark current density at forward bias ($V > V_{oc}$) is much lower than the value measured under solar light. This result indicates

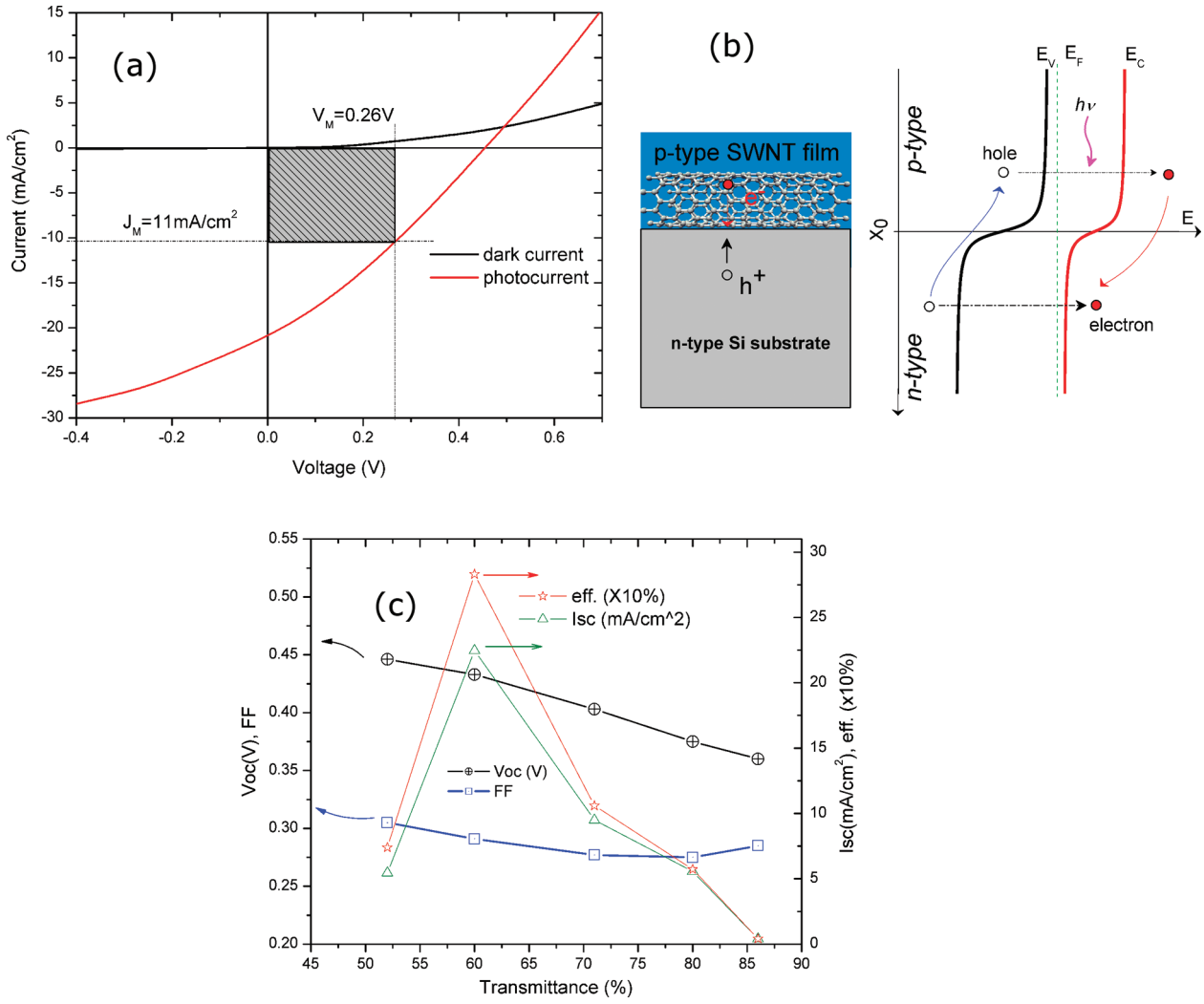

Figure 3. (a) Current−voltage plot of a typical SWNT/*n*-Si device under dark and illumination, showing typical solar cell performance with efficiency of 2.7%. (b) Schematic energy band diagram of a heterojunction diode showing the photogenerated carrier transfer process. (c) Summary of short-circuit current (J_{sc}), open-circuit voltage (V_{oc}), fill factor (f), and efficiency (η) for SWNT cells with different thickness, showing maximum current and efficiency of the device with transmittance of about 60%.

that light irradiation causes an increase in current at this voltage range (Figure 3a) and is consistent with previous observation on polymer/nanotube systems where optical excitation increases the current density at $V > V_{oc}$.[17] It should be noted that this behavior is in contrast to observed current reduction for double-wall carbon nanotube (DWNT) bundles under optical excitation.[18] The photoinduced current flows through DWNT bundles under irradiation at the visible region.[19] This current could be enhanced when light illuminates on the interface between the DWNTs and a metal electrode. SWNT films act as more efficient current carriers due to the much larger interfacial area created by the fully expanded SWNT films compared with thick DWNT bundles (where the DWNTs within the bundle do not contact directly the metal electrodes). The photoinduced electrons from SWNTs are injected to *n*-type Si substrate while holes are transported through the *p*-type SWNTs more efficiently. With 57% transmittance of the SWNT coating, the J_{sc} actually reaches 21.8 mA/cm^2 at AM1.5, much higher than that of the SWNT/metal junction. A Schottky junction made by a silver paste (to replace the SWNT film) on top of Si produced some power conversion, but the current density is 2 to 3 orders of magnitude lower (about several μA/cm^2) than the SWNT/*n*-Si junction.

The excellent photovoltaic performance of the SWNT solar cell originates from the creation of heterojunctions at the interface between the SWNT film and the *n*-Si substrate.[20] SWNTs usually behave as *p*-type semiconductors (also see the following Hall Effect measurement),[21] indicating that large amount of holes in SWNTs are available, consistent with earlier studies on field effect transistors made from carbon nanotubes.[22] When fully expanded on a planar Si substrate, there will be numerous *p*−*n* junctions formed due to close contact between SWNTs and underlying *n*-Si substrate. The *I*−*V* curve in the dark actually shows a typical diode behavior, further confirming the existence of *p*−*n* junction of this SWNTs-on-Si configuration (Figure 3a). The

rectifying behavior in the dark and the photocurrent phenomenon under illumination of the SWNT/*n*-Si heterojunction cell can be explained by the energy band structure of this heterostructure. Figure 3b shows the schematic energy band diagram of the heterojunction diode at thermal equilibrium. Since the band gaps (E_g) of our Si and SWNTs are 1.1 eV and less than 2.7 eV, respectively, an asymmetrical energy barrier would be formed at the junction interface. The holes and electrons generated in both sides of the heterojunction are effectively collected due to the large built-in electric field at the junction, where electrons are directed to the *n*-type Si region and holes are transported through the SWNTs. The resulting photocurrent is generated as schematically shown in Figure 3b. The high J_{sc} of the solar cells suggests that the presence of high density *p*−*n* junctions significantly enhanced the generation and transport of charge carriers from both SWNTs and silicon under light irradiation. Nanotubes act mainly as hole collectors and conductors in polymer/nanotube solar cells.[23] In our SWNT/*n*-Si devices, SWNTs might have participated in the photogeneration process as well as charge transport, and their high mobility ensures much enhanced efficiency compared with polymer composite cell structures. The high aspect ratios and large surface area of nanotubes could be beneficial to exciton dissociation and charge carrier transport, thus improving the overall power conversion efficiency.

The photocurrent generated by a solar cell under illumination at short circuit is dependent on the incident light. The photocurrent density can be related to the incident spectrum through the following equation:

$$J_{sc} = q \int b_s(\varepsilon)\, Q_E(\varepsilon)\, d\varepsilon \qquad (1)$$

where $b_s(\varepsilon)$ is the incident spectral photon flux density, the number of photons of energy in the range ε to $\varepsilon + d\varepsilon$ which are incident on unit area in unit time, and q is the electronic charge. Q_E depends upon the absorption coefficient of the solar cell material, the efficiency of charge separation, and the efficiency of charge collection in the device but does not depend on the incident spectrum. When the device is illuminated by simulated sunlight from the top of a *p*-type SWNT film, photons with energy less than E_g(SWNT) but greater than E_g(Si) will transmit through the SWNT films, acting as an optical "window", and be absorbed by the *n*-type Si substrate. Part of the light can directly reach the junction *via* the empty space between the SWNT networks. Simultaneously, light with photon energies larger than E_g(SWNT) will be absorbed by the SWNTs. In our case, the semiconducting tubes (6, 5) and (7, 5) dominate the tube species distribution, so only the photons with energies larger than the tubes' energy gaps and/or the silicon's energy gap can be absorbed and converted into electron−hole pairs (excitons). These results indicate that the *n*-Si substrate contributes to the absorption of most incident photons and to the production of charge carriers, which were subsequently diffused to the depletion region of the SWNT-Si junctions and separated.

The flexibility of the fabrication process allows for the construction of cell devices containing SWNT films with different thickness by controlling the airbrushing process. We have made cells with tailored SWNT film thicknesses ranging from 30 to about 270 nm (corresponding to 86−51% transmittance). All the cells show relatively stable voltages (V_{oc}) ranging from 0.37 to 0.45 V, but quite different current densities (J_{sc}) (Figure 3c). The cell with transmittance of 57% shows the highest J_{sc} (21.8 mA/cm^2) and η (2.7%, $\eta = fJ_{sc}V_{oc}/P_{input}$, where P_{input} is the incident power). At increased film thicknesses, the values of J_{sc} and η decrease significantly. Higher film thicknesses increase both the density of SWNTs and the total area of SWNT−Si junctions in the device, which could also enhance the current generation/transport. However, at a transmittance below 57% (thicker film), the SWNTs at the top layers are suspended on the underneath layers and cannot touch the Si substrate to form junctions. Also, thicker films are less transparent, and this prevents more incident light from reaching the substrate. Our results showed an optimal thickness of SWNT films that yielded about 57% transmittance, corresponding maximum current density, and efficiency. The fill factor and power efficiency of the SWNT/*n*-Si solar cell are about 0.29 and 2.7%, respectively (Figure 3c). Compared with previous solar cell configurations based on conjugated polymers mixed with SWNTs or double-walled nanotubes ($f \approx$ 15−30%, $\eta \approx$ 1%),[17] our devices show a fill factor in similar range but much higher efficiency. Our devices have the potential to be further optimized, for example, by tailoring the bundle size (dispersion) and the semiconducting to metallic tubes ratio of SWNTs. With these changes, power conversion efficiency can be further improved.

Enhanced Photovoltaic Effect by $SOCl_2$ Functionization. The conductivity of semitransparent SWNT thin films can be improved by a simple postdeposition method *via* exposure to nitric acid and thionyl chloride.[24] To enhance the performance of the solar cells, we carried out chemical doping using $SOCl_2$, a liquid organic solvent with remarkable reactivity toward the SWNTs surfaces. The $SOCl_2$ treatment involved dripping about 3 droplets of pure $SOCl_2$ onto the SWNT films followed by drying in air. The chemical attachments of functional groups to the SWNTs were in the form of acyl chloride groups. Figure 4a demonstrates the effect of the $SOCl_2$ treatment on the photovoltaic and electrical properties of a SWNT/*n*-Si device. After the $SOCl_2$ treatment, the short circuit current jumped to 26.5 from 20.7 mA/cm^2, and the open circuit voltage slightly increased to 0.49 from 0.46 V, and the *f* is raised up to 0.35 from 0.29. As a consequence of the $SOCl_2$ treatment, results showed a 59%

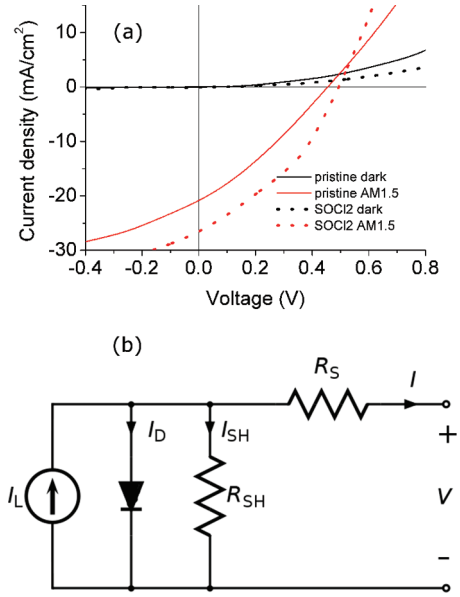

Figure 4. (a) The effect of the thionyl chloride ($SOCl_2$) treatment on the photovoltaic performance of SWNT/*n*-Si heterogeneous junctions. (b) The equivalent circuit of a solar cell. A solar cell may be modeled by a current source in parallel with a diode, R_{sh} and R_s are the shunt and series resistances, respectively.

increase in power conversion. Initial tests revealed a power conversion efficiency of about 4.5%.

The high conversion efficiency can be attributed to the high density $p-n$ junctions, which cause the formation of a strong built-in electric field and a wide photoactive region in our device. Photoactive regions for SWNT $p-n$ junctions are only near the narrow $p-n$ junction.[25] Another important reason for increased conversion is that the series resistances of the solar cells were reduced by the high density junctions. A qualitative explanation for the effect of series resistance can be understood from the equivalent circuit of the SWNT solar cell shown in Figure 4b. By neglecting the shunt resistance, R_{sh}, the actual short-circuit current in our devices can be expressed as

$$J_{SC} = J_{ph} - J_D = J_{ph} - J_S\left[\exp\left(\frac{q(J_{SC}R_S)}{mkT}\right) - 1\right] \quad (2)$$

where J_{ph} is the photocurrent, J_D is the forward biased current of the SWNT solar cell, J_S is the reverse saturation current, R_S is the sum of the series resistances of the SWNT solar device (the effective total of the contact resistances and the nanotube resistances), and q, m, k, and T are the electron charge, ideality factor, Boltzmann's constant, and absolute temperature, respectively. In most traditional Si solar cells R_S is small enough so that its effect is negligible, while in the SWNT solar cells, R_S is large and needs to be considered. If no further post treatment is done for the contacts, R_S could reach up to tens of megaohms for individual SWNT diodes.[26] By fitting the dark $I-V$ curve of the device with the following diode equation,

$$J = J_S\left[\exp\left(\frac{q(V - JR_S)}{mkT}\right) - 1\right] \quad (3)$$

where J and V are the diode current and biasing voltage, respectively, the series resistance was found to be about 21 Ω in the pristine solar cell and about 16 Ω in the $SOCl_2$-treated device. According to eq 2, J_{SC} is largely enhanced with a significant decrease of R_S. Thus, the efficiency can be effectively improved. The value of *Rs* can be further decreased by reducing the SWNT film resistance, and improving the electrical contacts at the top (SWNT) and bottom (Si) sides.

The conduction mechanism of the SWNT coating films can be understood from the DC conductivity behaviors at low temperatures (Figure 5a). Two major mechanisms responsible for the conductivity−temperature dependence of the CNT network films are (1) fluctuation-assisted tunneling[27] through barriers, with the order of magnitude of typical energies indicated by the value of k_BT_b and extent of the decrease of conductivity at low temperatures is indicated by the ratio T_s/T_b; (2) hopping between mesoscopic metallic islands of conducting tubes separated by insulating tubes, following Mott's variable-range hopping law for disordered semiconductors.[28] So, the temperature dependence of conductance can be expressed in the following form:[29]

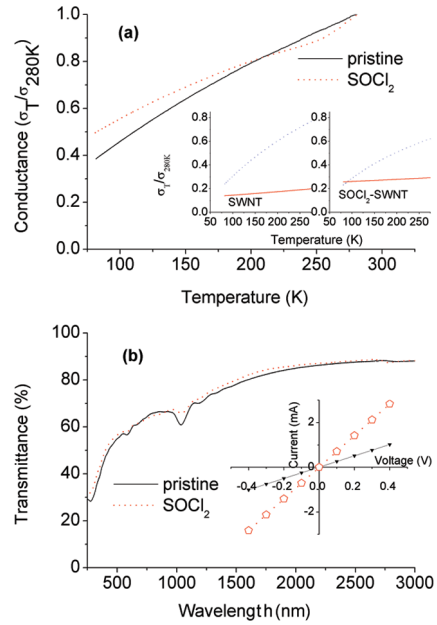

Figure 5. (a) Normalized temperature dependent conductances of semitransparent carbon nanotube coating films. The inset displays the two main conductance contributions: variable range hopping (blue dash) and fluctuation-assisted tunneling (red solid). (b) Effect of the $SOCl_2$ treatment on the electron transportability and optical properties of the SWNT film. The inset exhibits the four-probe $I-V$ curves taken on the SWNT film with 57% transmittance before (black triangle) and after (red pentagon) $SOCl_2$ treatment, indicating a decrease in sheet resistance by a factor of ~3.

$$\sigma(T) = \sigma_t e^{-T_b/(T_s+T)} + \sigma_0 e^{-(T_0/T)^{1/2}} \quad (4)$$

where the geometrical factors σ_t and σ_0 can be treated as constant. For the present cases we take T_b and T_0 as constants. As the principal mechanism of electrical conduction in the CNT networks, the variable-range hopping between CNTs is more sensitive to the temperature change than the fluctuation-assisted tunneling. Although the SWNT material might contain a small fraction of metallic nanotubes, both pristine and $SOCl_2$-treated SWNT networks show nonmetallic behavior, suggesting the presence of tunneling barriers at the intertube junctions,[30,31] with much stronger suppression of electron tunneling in the case of pristine SWNT film. But for the films with medium thickness (*e.g.*, those at ~57% transparency, shown here), the variable-range hopping contributes more to the conductance behavior than the thermal fluctuation-assisted tunneling does (Figure 5a, inset). A crossover behavior was observed above 250 K in the $SOCl_2$-treated SWNT film. Crossover can be explained with the interrupted metallic model in which carriers of quasi-1D conductors cannot circumvent defects or other barriers (such as functional groups). As temperature increases, thermal fluctuations assist the tunneling and increase the conductance. At higher temperatures, the usual decrease in conductivity due to scattering of carriers by photons may dominate the temperature dependence.[32]

The conductivity of the pristine SWNT films can be significantly increased by $SOCl_2$-treatment. As a strong oxidizing agent, $SOCl_2$ exhibits remarkable electron-withdrawing ability when adsorbed onto the SWNT surface.The significant charge transfer induced by $SOCl_2$ could also enable Fermi level shifting into the van Hove singularity region of SWNTs, resulting in a substantial increase in the density of states near the Fermi level. With this functioning technique, typical sheet conductance of the SWNT films can be improved 3−10-fold. The treatment with $SOCl_2$ also weakens the S_{11} (S_{22}) interband transition between the first (second) pair of van Hove singularities of the semiconducting tubes. Additionally, the $SOCl_2$ modification could be responsible for the generation of small gaps in the metallic SWNTs, which determines the far IR absorption band (Figure 5b). The transparency is considerably higher at energies below 1.1 eV (~1100 nm), which is where the optical transparency of traditional ITO degrades due to free-carrier absorption. Higher transparency at long wavelengths combined with higher conductivity would be a beneficial property for the thin-film tandem solar cells.[33] In our configuration, SWNTs act as photogenerators as well as charge transporters. Semiconducting tubes would improve the photogeneration process but would exhibit poor conductivity; on the contrary, metallic tubes would contribute to more charge transportation but less photogeneration. Since $SOCl_2$ treatment can significantly improve the conductivity of semiconducting SWNT film, metallic tubes play a less important role in the photoconversion of the $SOCl_2$-enhanced SWNT/*n*-Si device.

Carrier densities and mobilities of these CNT films can be determined by Hall-effect measurements. The concentration of the carriers is given in terms of the sheet number N_{2D} (cm^{-2}). After $SOCl_2$-treatment, the carrier densities for the CNT films increased from 3.1×10^{15} to 4.6×10^{17} cm^{-2}. The effective mobilities for the SWNT, $SOCl_2$−SWNT films and *n*-Si are 2.1, 17.2, and 1026 $cm^2\ V^{-1}\ s^{-1}$, respectively. Interestingly, the $SOCl_2$ treatment can also significantly enhance the SWNT mobility. The low mobility of the SWNT network could be caused by several factors including high resistivity between SWNT bundles and Schottky barriers between semiconducting and metallic nanotubes.[34] The Hall effect measurements show that all CNT film samples show *p*-type conductivity. The acid reflux-based purification procedures can often beneficially dope the *p*-type semiconducting tubes.[35] This, along with doping from atmospheric impurities,[36] is thought to influence the optoelectronic performances of the films. Transparent electrical CNT films are hole conducting, simple to deposit, flexible, and low cost. Hence, they would be highly beneficial for the next generation of solar cells.

CONCLUSION

High density SWNT/*n*-Si heterojunctions prepared with a simple airbrushing technique show a strong rectifying behavior and photovoltaic effects during optical excitation. The SWNTs in the cells are involved in multiple processes that are critical in improving the efficiency, including charge separation, transport, and collection. The numerous heterojunctions formed between *p*-SWNTs and *n*-Si substrate perform similar to the conventional *p*−*n* junctions in the generation of electron−hole pairs, which then split and transported through SWNTs (holes) and *n*-Si substrate (electrons), respectively. After the $SOCl_2$ treatment, the major conduction mechanism of the SWNT coating network shifts from hopping towards tunneling. The $SOCl_2$ treatment of SWNT films also leads to significant increases in the conversion efficiency by adjusting the Fermi level and enhancing the carrier mobility of the SWNT coatings. The larger carrier density and higher mobility of $SOCl_2$-treated SWNTs ensure more enhanced current density and power conversion efficiency of solar cells compared with extensively studied polymer-nanotube composite structures. We believe the photoconversion efficiency of our devices can be further improved, for example, by optimizing the dispersion and thickness of the SWNT film, the *n*-doping level of the Si substrate, and the efficient electrode design for charge collection.

EXPERIMENTAL SECTION

Fabrication of SWNT/*n*-Si Heterojunctions. The small diameter SWNTs were synthesized from CO proportionation over a

Co−Mo/SiO_2 catalyst.[37] SWNTs consist of seamlessly rolled-up graphene sheets of carbon with π-conjugated and highly hydrophobic sidewalls but can interact with, for example, surfactants and some kinds of aromatic compounds through hydrophobic or π−π electronic interaction(s).[38] Therefore, the CNTs can be made into uniform solutions with proper treatment. The purified CNTs were first dissolved in dimethylformamide (DMF, 0.5 mg/mL) under sonication, and the uniform solution was directly sprayed onto *n*-type silicon wafers and glass substrates (for reference) by means of an airbrush using dry air as carrier gas at 2 bar. A silicon wafer with a window of predeposited insulating layer and a glass substrate were placed on a heating platform side by side so that the resulting SWNT network films on *n*-Si and glass substrates has the same thickness. This assembly was then heated up to 150 °C in order to evaporate DMF solvent from the film and prepare it for further characterization.

Materials and Devices Characterization. Optical transmission was chosen as an appropriate method of averaging the structural irregularities and characterizing the thickness of various thin SWNT networks prepared on a glass substrate, using a Shimadzu double beam spectrophotometer UV-3600 with three detectors, in the range of wavelengths from 200 to 3300 nm. The temperature dependent conductivity measurements were performed for the reference SWNT films. Electrical resistivity data as a function of temperature was obtained using a Keithley 2000 digital multimeter connected to a four-probe collinear arrangement on the thin film square samples 5 × 5 mm^2 with parallel silver contacts. The contacts showed a good Ohmic behavior for all samples. The observed temperature gradient across the sample was typically 1−2 K and monitored by a silicon diode thermosensor. The Hall Effect measurements were performed under a magnetic field of 0.2 T by using standard Van der Pauw geometry. To perform the photovoltaic testing, the devices were irradiated under a small-area class-B solar simulator (PV Measurements, Inc.) at AM1.5 (~100 mW/cm^2). Data were recorded using a Keithley 2400.

Acknowledgment. This research was partially supported by the DOE (Grant No. DE-FG 36-06 GO 86072). The financial support from Arkansas Science and Technology Authority (ASTA) Grant No. 08-CAT-03 is highly appreciated.

Note added after ASAP publication: An older version of Figure 4 was published with this article May 20, 2009. The correct figure was reposted May 29, 2009.

REFERENCES AND NOTES

1. Avouris, P. Carbon Nanotube Electronics and Optoelectronics. *MRS Bull.* **2004**, *29*, 403–410.
2. Dervishi, Enkeleda; Li, Zhongrui; Xu, Yang; Saini, Viney; Biris, Alexandru R.; Lupu, Dan; Biris, Alexandru S. Carbon Nanotubes: Synthesis, Properties, and Applications. *Part. Sci. Technol.* **2009**, *27* (2), 107–125.
3. Lee, J. U. Photovoltaic effect in ideal carbon nanotube diodes. *Appl. Phys. Lett.* **2005**, *87*, 073101/1–073101/3.
4. Ago, H.; Petritsch, K.; Shaffer, M. S. P.; Windle, A. H.; Friend, R. H. Composites of Carbon Nanotubes and Conjugated Polymers for Photovoltaic Devices. *Adv. Mater.* **1999**, *11*, 1281–1285.
5. Kymakis, E.; Amaratunga, G. A. J. Single-Wall Carbon Nanotube/Conjugated Polymer Photovoltaic Devices. *Appl. Phys. Lett.* **2002**, *80*, 112–114.
6. Bhattacharyya, S.; Kymakis, E.; Amaratunga, G. A. J. Photovoltaic Properties of Dye Functionalized Single-Wall Carbon Nanotube/Conjugated Polymer Devices. *Chem. Mater.* **2004**, *16*, 4819–4823.
7. Kymakis, E.; Koudoumas, E.; Franghiadakis, I.; Amaratunga, G. A. J. Post-fabrication Annealing Effects in Polymer-Nanotube Photovoltaic Cells. *J. Phys. D: Appl. Phys.* **2006**, *39*, 1058–1062.
8. Miller, A. J.; Hatton, R. A.; Chen, G. Y.; Silva, S. R. P. Carbon Nanotubes Grown on In_2O_3:Sn Glass as Large Area Electrodes for Organic Photovoltaics. *Appl. Phys. Lett.* **2007**, *90*, 023105/1–023105/3.
9. O'Connell, M. J.; Bachilo, S. M.; Huffman, C. B.; Moore, V. C.; Strano, M. S.; Haroz, E. H.; Rialon, K. L.; Boul, P. J.; Noon, W. H.; Kittrell, C.; *et al.* Band Gap Fluorescence from Individual Single-Walled Carbon Nanotubes. *Science* **2002**, *297*, 593–596.
10. Hagen, A.; Hertel, T. Quantitative Analysis of Optical Spectra from Individual Single-Wall Carbon Nanotubes. *Nano Lett.* **2003**, *3*, 383–388.
11. Pedersen, T. G. Variational Approach to Excitons in Carbon Nanotubes. *Phys. Rev. B* **2003**, *67*, 073401/1–073401/4.
12. Odom, T. W. O.; Huang, J. L.; Kim, P.; Lieber, C. M. Atomic Structure and Electronic Properties of Single-Walled Carbon Nanotubes. *Nature* **1998**, *391*, 62–64.
13. Fuhrer, M. S.; Kim, B. M.; Du1rkop, T.; Brintlinger, T. High-Mobility Nanotube Transistor Memory. *Nano Lett.* **2002**, *2*, 755–759.
14. Freitag, M.; Perebeinos, V.; Chen, J.; Stein, A.; Tsang, J. C.; Misewich, J. A.; Martel, R.; Avouris, P. Hot Carrier Electroluminescence from a Single Carbon Nanotube. *Nano Lett.* **2004**, *4*, 1063–1066.
15. Bachilo, S. M.; Balzano, L.; Herrera, J. E.; Pompeo, F.; Resasco, D. E.; Weisman, R. B. Narrow (*n*,*m*)-Distribution of Single-Walled Carbon Nanotubes Grown Using a Solid Supported Catalyst. *J. Am. Chem. Soc.* **2003**, *125*, 11186–11187.
16. Somani, S. P.; Somani, P. R.; Umeno, M.; Flahaut, E. Improving Photovoltaic Response of Poly(3-hexylthiophene)/n-Si Heterojunction by Incorporating Double-Walled Carbon Nanotubes. *Appl. Phys. Lett.* **2006**, *89*, 223505/1.
17. Pradhan, B.; Batabyal, S. K.; Pal, A. J. Functionalized Carbon Nanotubes in Donor/Acceptor-Type Photovoltaic Devices. *Appl. Phys. Lett.* **2006**, *88*, 093106/1–093106/3.
18. Wei, J. Q.; Sun, J. L.; Zhu, J. L.; Wang, K. L.; Wang, Z. C.; Luo, J. B.; Wu, D. H.; Cao, A. Y. Carbon Nanotube Macrobundles for Light Sensing. *Small* **2006**, *2*, 988–993.
19. Sun, J. L.; Wei, J. Q.; Zhu, J. L.; Xu, D.; Liu, X.; Sun, H.; Wu, D. H.; Wu, N. L. Photoinduced Currents in Carbon Nanotube/Metal Heterojunctions. *Appl. Phys. Lett.* **2006**, *88*, 131107/1–131107/3.
20. Wei, J.; Jia, Y.; Shu, Q.; Gu, Z.; Wang, K.; Zhuang, D.; Zhang, G.; Wang, Z.; Luo, J.; Cao, A.; Wu, D. Double-Walled Carbon Nanotube Solar Cells. *Nano Lett.* **2007**, *7* (8), 2317–2321.
21. Shimada, T.; Sugai, T.; Ohno, Y.; Kishimoto, S.; Mizutani, T.; Yoshida, H.; Okazaki, T.; Shinohara, H. Double-Wall Carbon Nanotube Field-Effect Transistors: Ambipolar Transport Characteristics. *Appl. Phys. Lett.* **2004**, *84*, 2412–2414.
22. Martel, R.; Schmidt, T.; Shea, H. R.; Hertel, T.; Avouris, P. Single- and Multi-wall Carbon Nanotube Field-Effect Transistors. *Appl. Phys. Lett.* **1998**, *73*, 2447–2449.
23. Pasquier, A. D.; Unalan, H. E.; Kanwal, A.; Miller, S.; Chhowalla, M. Conducting and Transparent Single-Wall Carbon Nanotube Electrodes for Polymer-Fullerene Solar Cells. *Appl. Phys. Lett.* **2005**, *87*, 203511.
24. Parekh, B. B.; Fanchini, G; _Eda, G.; Chhowalla, M. Improved Conductivity of Transparent Single-Wall Carbon Nanotube Thin Films *via* Stable Postdeposition Functionalization. *Appl. Phys. Lett.* **2007**, *90*, 121913/1–121913/3.
25. Stewart, D. A.; Leonard, F. Energy Conversion Efficiency in Nanotube Optoelectronics. *Nano Lett.* **2005**, *5*, 219–222.
26. Chen, C. X.; Yan, L. J.; Kong, E. S. W.; Zhang, Y. F. Ultrasonic Nanowelding of Carbon Nanotubes to Metal Electrodes. *Nanotechnology* **2006**, *17*, 2192–2197.
27. Sheng, P. Fluctuation-Induced Tunneling Conduction in Disordered Materials. *Phys. Rev. B* **1980**, *21*, 2180–2195.
28. Ehinger, K.; Roth, S. Non-solitonic Conductivity in Polyacetylene. *Philos. Mag. B* **1986**, *53*, 301–320.
29. Kaiser, A. B. Electronic Transport Properties of Conducting Polymers and Carbon Nanotubes. *Rep. Prog. Phys.* **2001**, *64*, 1–49.
30. Hone, J.; Llaguno, M. C.; Nemes, N. M.; Johnson, A. T.; Fischer, J. E.; Walters, D. A.; Casavant, M. J.; Schmidt, J.;

Smalley, R. E. Electrical and Thermal Transport Properties of Magnetically Aligned Single Wall Carbon Nanotube Films. *Appl. Phys. Lett.* **2000**, *77*, 666.
31. Gruner, G. Carbon Nanotube Films for Transparent and Plastic Electronics. *J. Mater. Chem.* **2006**, *16*, 3533–3539.
32. Kaiser, A. B. Systematic Conductivity Behavior in Conducting Polymers: Effects of Heterogeneous Disorder. *Adv. Mater. (Weinheim, Ger.)* **2001**, *13*, 927–941.
33. Coutts, T. J.; Ward, J. S.; Young, D. L.; Emery, K. A.; Gessert, T. A.; Noufi, R. Critical issues in the design of polycrystalline, thin-film tandem solar cells. *Prog. Photovoltaics* **2003**, *11*, 359–375.
34. Stadermann, M.; Papadakis, S. J.; Falvo, M. R.; Novak, J.; Snow, E.; Fu, Q.; Liu, J.; Fridman, Y.; Boland, J. J.; Superfine, R.; Washburn, S. Nanoscale Study of Conduction through Carbon Nanotube Networks. *Phys. Rev. B* **2004**, *69*, 201402/1–201402/3.
35. Skakalova, V.; Kaiser, A. B.; Dettlaff-Weglikowska, U.; Hrncarikova, K.; Roth, S. Effect of Chemical Treatment on Electrical Conductivity, Infrared Absorption, and Raman Spectra of Single-Walled Carbon Nanotubes. *J. Phys. Chem. B* **2005**, *109*, 7174–7181.
36. Collins, P. G.; Bradley, K.; Ishigami, M.; Zettl, A. Extreme Oxygen Sensitivity of Electronic Properties of Carbon Nanotubes. *Science* **2000**, *287*, 1801–1804.
37. Alvarez, W. E.; Pompeo, F.; Herrera, J. E.; Balzano, L.; Resasco, D. E. Characterization of Single-Walled Carbon Nanotubes (SWNTs) Produced by CO Disproportionation on Co−Mo Catalysts. *Chem. Mater.* **2002**, *14*, 1853–1858.
38. Richard, C.; Balavoine, F.; Schultz, P.; Ebbesen, T. W.; Mioskowski, C. Supramolecular Self-Assembly of Lipid Derivatives on Carbon Nanotubes. *Science* **2003**, *300*, 775–778.